Fully Printed Electrolyte-Gated Transistor Formed in a 3D Polymer Reservoir with Laser Printed Drain/Source Electrodes

Gabriel Cadilha Marques,* Liang Yang, Yan Liu, Vanessa Wollersen, Torsten Scherer, Ben Breitung, Martin Wegener, and Jasmin Aghassi-Hagmann*

In solution processed electronic devices it is crucial that the deposited inks are properly aligned and that all post-processing steps are compliant with each other. Moreover, shorter channel lengths are highly beneficial to increase the device performance. Herein, laser printing of metals and polymer reservoirs allows to print sub-micrometer sized channel lengths while confining functional inks into these small gaps. Therefore, a manufacturing concept and optimized material stack, suitable for combined inkjet and laser printing are proposed. A nanoparticulate indium oxide (In_2O_3) semiconductor is inkjet printed into and constrained by a 3D laser written polymer (pentaerythritol triacrylate, PETA) reservoir. Inside the 3D printed polymer reservoir, platinum (Pt) electrodes, that are further routed over the reservoir walls, are laser printed by a metal reduction process. The transistor fabrication is completed by a second inkjet printed layer of composite solid polymer electrolyte and an organic top-gate layer (PEDOT:PSS). This concept does not exceed annealing temperatures higher than 100 °C, and is compatible with a range of substrates. The characterized electrolyte-gated field-effect transistor show a reasonable on/off-ratio in the range of 10^4 with negligible leakage currents. This materials and hybrid device manufacturing scheme has believed great potential for bioelectronics, lab-on-a-chip applications and others.

1. Introduction

Over the past decade, applications in the field of printed electronics have become more mature due to material improvements and optimizations in fabrication techniques.[1] Typically, in printed electronics, the manufacturing is based on an additive process.[2] The main advantage of an additive manufacturing process is that functional materials are deposited on top of each other and on demand. Additive manufacturing comes along with the benefits of cost-efficiency, reduced material consumption, and support for high-throughput fabrication.[3,4] The materials themselves are formulated by functional inks and can be deposited with the help of inkjet, aerosol, electrohydrodynamic, laser, or other 2D/3D printing techniques.[5–7] During the printing of electronic devices and circuits, it might be important that some of the functional materials are in contact with each other

G. Cadilha Marques, L. Yang[+], Y. Liu, V. Wollersen, T. Scherer,
B. Breitung, M. Wegener, J. Aghassi-Hagmann
Institute of Nanotechnolgy
Karlsruhe Institute of Technology
Herman-von-Helmholtz-Platz 1, 76344 Eggenstein-Leopoldshafen,
Germany
E-mail: gabriel.marques@kit.edu; jasmin.aghassi@kit.edu

L. Yang[+], M. Wegener
Institute of Applied Physics (APH)
Karlsruhe Institute of Technology (KIT)
Wolfgang-Gäde-Straße 1, 76128 Karlsruhe, Germany
V. Wollersen, T. Scherer
Karlsruhe Micro Nano Facility (KMNFi)
Eggenstein-Leopoldshafen Research Center
Wolfgang-Gäde-Straße 2, 76344 Eggenstein-Leopoldshafen, Germany

to form an electronic contact. On the other hand, unintentional electronic contacts between the functional materials can lead to short-circuits.[8] Therefore, one critical challenge during printing is to control the spreading of the ink on the substrate and to deposit the material solely at the desired intended location.

Using assistive capillary structures, it is in general possible to control the flow of an ink on a substrate.[9] In this regard, capillary-assist structures (CASs) are imprinted on a substrate by immersing a stamp that contains the CASs into a dispersion consisting of a polymer upon which the CASs are based. After pressing the coated stamp on the substrate and a subsequent hardening step, the stamp is removed from the substrate leaving the CASs behind. Another method to imprint CASs, is by placing a pristine stamp on a substrate and filling the structures with a polymer dispersion. Thereafter, the polymer dispersion is hardened, the stamp is peeled off, and the CASs remain on the substrate.[10] Furthermore, CASs can also be imprinted on a substrate by coating a substrate with a polymer dispersion and pressing a stamp that contains the negative of the CASs. Finally, in this case, the CASs stick to the substrate after solidifying the polymer dispersion and removing the stamp.[10,11] With the help of these CASs, electronic components can be printed. Thereby, the functional inks are printed into reservoirs and guided through capillaries to the desired location on the substrate.[12] This allows the functional inks to be confined within certain borders and reliable electrically contact various devices without creating short- or open-circuits. However, placing capillaries on a substrate requires additional complex fabrication steps, which are beyond additive manufacturing. The complexity in fabrication is related to the fact that the stamps are fabricated in a subtractive manner that involve several lithography steps.[11,12] In addition, whenever dimensions of a printed device or the design of a circuit change, new stamps need to be fabricated, forming a major drawback.

Here, the idea of filling reservoirs with functional inks is translated to building electronic devices. An additive mulit-photon laser printing method[13–15] is used to write polymer reservoirs directly on the substrate. This reduces the fabrication complexity because the previously discussed stamps are obsolete. Furthermore, the reservoir itself fulfills two functionalities. First, the reservoir confines the inkjet printed ink within the desired area. Second, conductive structures are laser printed on the inner part of the reservoir, allowing this inner part to be used as a conductive electrode. Therefore, there are no capillaries connected to the reservoir and the electronic components can be directly constructed inside the reservoir. A conductive platinum (Pt) electrode is then wired outside the reservoir, by laser printing Pt lines over the polymer reservoir, to electrically connect the device to contact pads. The reservoir is a crucial element of the electronic device and is not just a container that holds the ink within a certain area, as it is typically found in literature.

The main benefit of the proposed reservoirs is that the electronic contact between the functional ink and the metal electrode is improved. Moreover, the functional inks are confined within the desired area even if the designs contain structures below the critical printing resolution of 10 μm. However, in a transistor, the reservoir can help to form a vertical contact with the semiconductor. Such a 3D vertical contact extends the planar transistor into the third dimension. A 3D contact does not only reduce the footprint of transistors but also reduces their variability

in terms of electrical characteristics because the contact area is increase, improving the interface between the electrode and the material which is filled into the reservoir.[16–18] In addition, integrating electronic devices into the reservoir could become interesting in future for bioelectronic applications, where a specimen is filled into the reservoir and is directly evaluated by the electronics integrated into the reservoir.
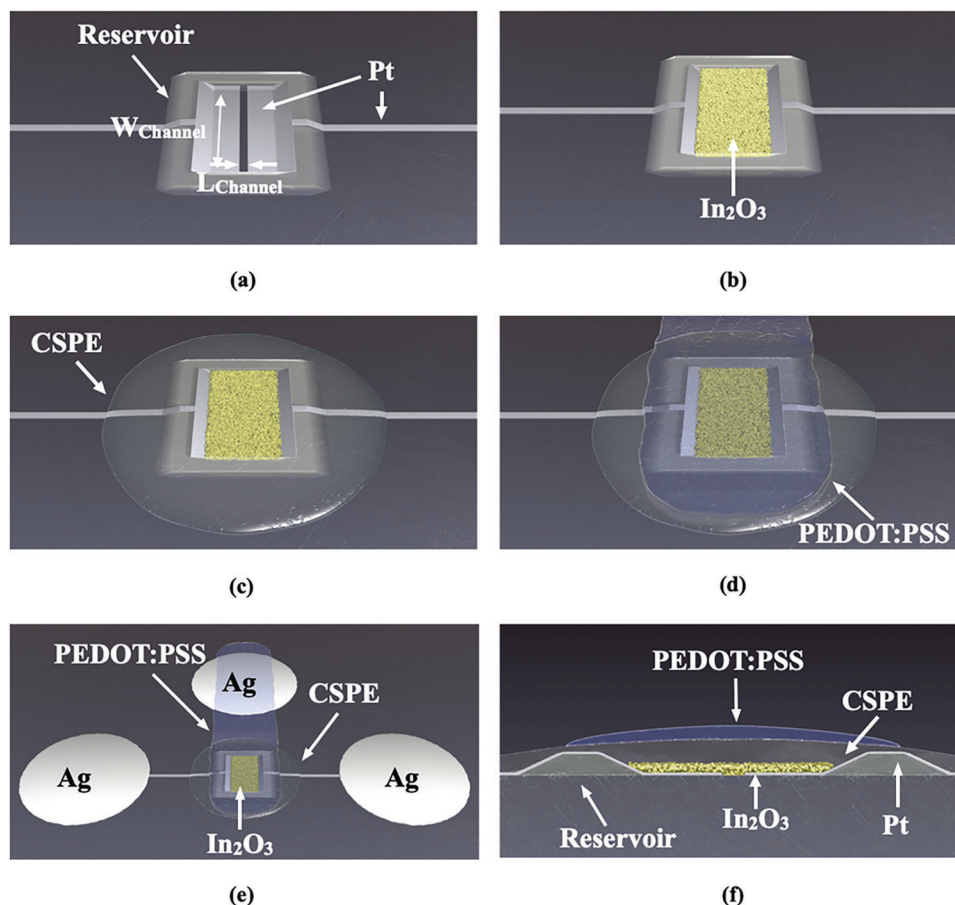
2. Results and Discussion

The focus of this paper lies on electrolyte-gated field-effect transistors (EGTs) with lateral 3D metal drain- and source-electrodes. The main part of the EGT is the reservoir, with the inner part of the deposited with Pt, that is filled with functional inks. A gap is present in the center of the reservoir, which defines the channel length ($L_{channel}$) of the EGT and the horizontal distance between the inner sidewalls is the channel width ($W_{channnel}$) (**Figure 1**a). To electrically contact the EGT, two Pt wires are printed to the drain- and source-electrodes, respectively. In the second step, indium oxide (In_2O_3) nanoparticles are printed into the reservoir and act as the channel material (Figure 1b). Next, a composite solid polymer electrolyte (CSPE) is printed on top of the reservoir as the gate-isolator (Figure 1c), followed by the top-gate electrode (PEDOT:PSS) (Figure 1d). Additionally, silver (Ag) contact pads are printed to allow for electrical measurements (Figure 1e). In Figure 1f, the cross-section of the reservoir area is depicted. It is worth mentioning that the polymer reservoir and the Pt are deposited through a direct laser writing method. Alternatively, the In_2O_3 nanoparticles, the CSPE, the PEDOT:PSS, and the Ag structures are inkjet printed with the Dimatix MP 280 material inkjet printer.

2.1. Laser Printed Polymer Reservoir and Metal Electrodes

Before discussing the characteristics of the EGT, the manufacturing process of the reservoir is presented in more detail. To realize a 3D polymer reservoir with metal electrodes, a multi-material laser printing method is introduced in this study. Thereby, a combination of multi-photon polymerization for the polymer reservoir and multi-photon reduction for the metal electrodes is shown. The printing procedure is illustrated in **Figure 2**a. In the first step, the 3D polymer structure is printed using an electrically isolating pentaerythritol triacrylate (PETA) photoresist. The polymer structure acts as a substrate for further deposition of metal electrodes. After washing the unexposed photoresist away, the polymer structure is immersed in a Pt ink for further printing of conductive Pt electrodes. Laser printing of Pt metal structures has recently been investigated in detail.[19,20] The Pt-ink in this work is prepared from a Pt(II) salt dissolved in water with an iron(III) oxalate as photosensitizer.

By focusing a femtosecond laser into the Pt-ink, Pt-ions are reduced by multi-photon-absorption. Thus, Pt nanoparticles are formed and aggregate together. In the Pt printing process, light-induced forces onto the metal nanoparticles play a critical role for nanoparticles aggregation.[19] The aggregated Pt nanoparticles are sintered together on the substrate surface by laser-induced local heating, forming solid Pt structures. The large difference in

**ADVANCED
SCIENCE NEWS**

www.advancedsciencenews.com

**ADVANCED
MATERIALS
TECHNOLOGIES**

www.advmattechnol.de

Figure 1. Manufacturing scheme of the 3D hybrid electrolyte-gated transistor (EGT) consisting of two laser printing steps and four inkjet printing steps. a) Laser printed polymer reservoir (90 µm × 90 µm) with the laser written Pt inner electrodes and wire connections ranging over 5 µm polymer walls. b) In_2O_3 nanoparticle ink printed into the reservoir/electrode structure. c) The composite solid polymer electrolyte (CSPE) is inkjet printed over the In_2O_3 film. d) PEDOT:PSS is printed on the CSPE as a top gate-electrode. e) Finally obtained EGT with inkjet printed silver (Ag) contact pads outside the polymer reservoir. f) Graphical representation of the cross-section of the reservoir area of the EGT.

thermal conductivity of Pt structures and the surrounding aqueous ink limits the heating area below a micrometer.[21,22]

Pt lines can be printed, both, on the surfaces of the glass substrate and the polymer structure, respectively, resulting in continuous and conductive metal electrodes. Since the polymer reservoir is a 3D object and partially with Pt, 3D metal electrodes are formed this way. Finally, the 3D metal electrodes, which are finally cleaned in water and dried with nitrogen.

To demonstrate the capability of the 3D metal electrodes printing, various Pt patterns are written on different faces of a 3D pyramid polymer structure (Figure 2b). A continuous Pt line extending from the glass substrate over the pyramid structure and finally ending again on the glass substrate is also shown in Figure 2c. Similarly, 3D Pt lines can be printed to connect the inner and outer sides of the polymer reservoir (Figure 2d), to be able to electrically contact the inner structures of the reservoir. The polymer reservoir and the Pt pattern can be flexibly designed with sub-micrometer feature sizes through the same laser printing system.

A Pt deposited reservoir structure as shown in Figure 2e is adopted for fabricating the EGT. The whole polymer structure is 90 µm × 90 µm in area with a slope of 45° along the horizontal di-

rection. The bottom side of the inner reservoir is 70 µm × 40 µm in area. The inner sidewalls and the bottom of the reservoir are completely covered with a layer of Pt, leaving a gap of 3 µm behind, which separates the Pt electrodes into drain- and source-electrodes for EGT. The inner Pt layers are wired to the outside world by two Pt lines (5 µm width) on the left and the right-hand side. The optical image of the polymer reservoir covered with Pt is shown in Figure 2e. The SEM images of the reservoir area and the gap are depicted in Figure 2f,g.

Benefiting from the flexibility of the additive laser printing, the morphology of the polymer reservoir and the conductive metal layer can be adjusted according to the specific requirements. Beyond the reservoir presented in Figure 2e-g, other reservoirs covered with Pt structures have also been fabricated (Figure S1, Supporting Information). The conductivity of the Pt structures play a critical role in the performance of the final EGT. For the conductivity test, the morphology of a single Pt wire is measured with atomic-force microscopy (AFM), and the voltage-current curve collected by a probe station reveals a high conductivity of ~1/10 of bulk Pt (Figure S2, Supporting Information).

However, the parameters of metal printing need to be well controlled to realize continuous and solid Pt structures on polymer
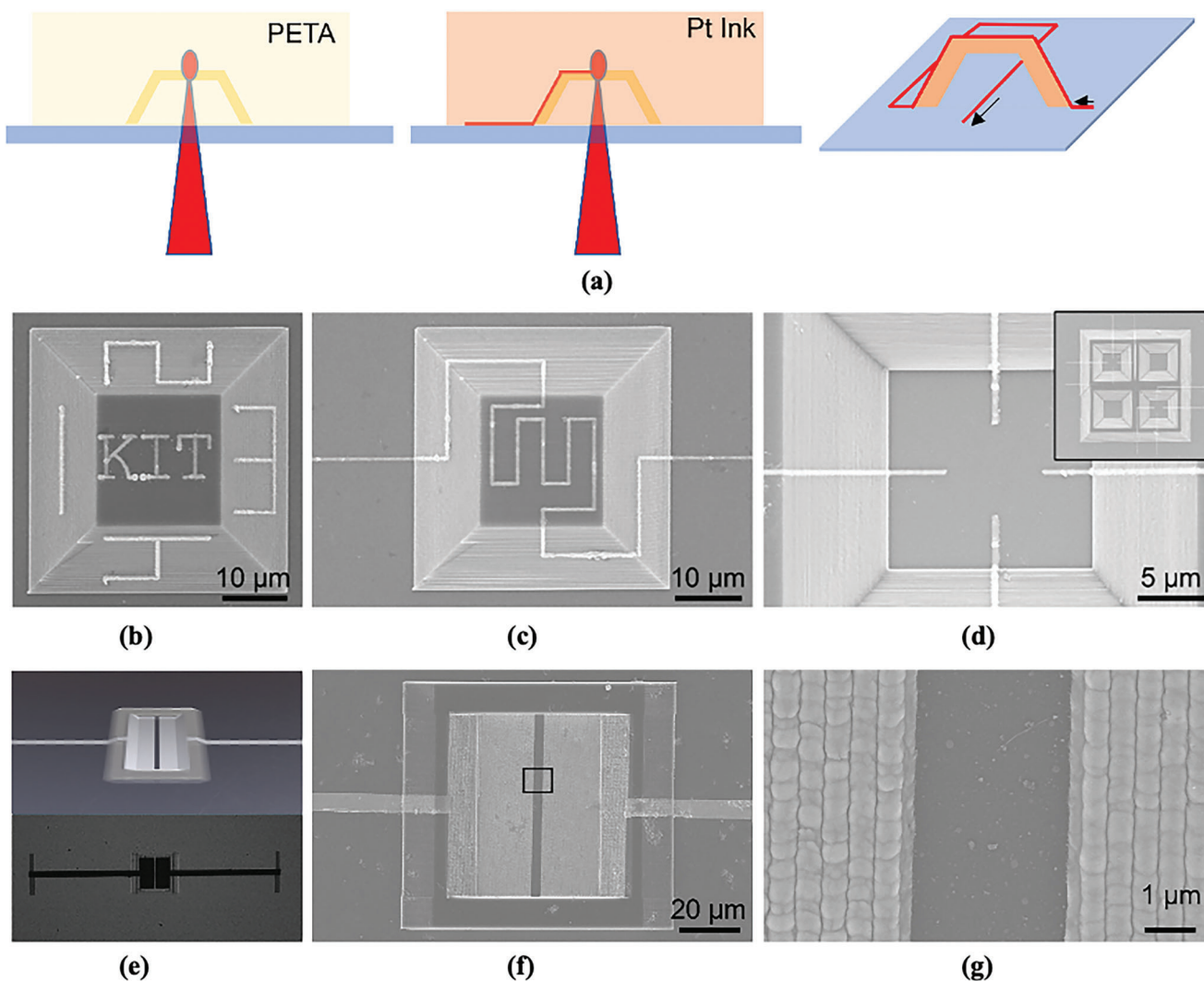
Figure 2. Direct laser printing of polymer reservoir and metal electrodes. a) Procedures of the laser printing process. b) Pt patterns printed over different faces of a 3D pyramid scaffold. c) Continuous 3D conductive Pt line printed over pyramid scaffold. d) 3D conductive Pt line extended inside polymer reservoir. e) Schematic and optical image of the metal deposited polymer reservoir used in this study. SEM images of the f) the reservoir area g) and the channel area between source- and drain-electrodes.

and on glass surfaces. By repeated experiments, we find that the laser focus velocity should be slower than $10\,\mu m^{-1}s$, and the laser power should be modulated within a specific window at fixed velocity (Figure S3, Supporting Information). Outside this power window, the laser is either too weak to induce the metal printing process or too strong such that the heat accumulation tends to damage the printed structures.
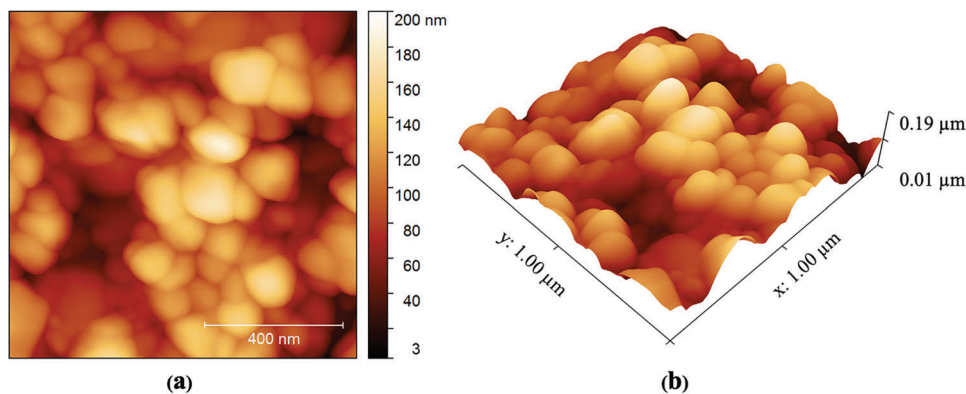
2.2. Inkjet Printed Channel

Later, a reservoir will be partially filled with In_2O_3 nanoparticles, to fabricate an EGT, which demonstrates the great potential of these reservoirs for printed electronic applications. Thereby, In_2O_3 nanoparticles act as an *n*-type semiconducting channel. Due to the high carrier mobility and density of bulk In_2O_3[23], this semiconductor is chosen as the channel material of the EGT.

For In_2O_3 based printed filed-effect transistors, depending on the film morphology and annealing conditions, field-effect mobility values between 5 and 200 cm^2 (Vs^{-1}) are reported in the literature.[24–26]

Typically, the indium oxide film needs to be annealed at a high temperature (>300°C), to achieve the aforementioned high carrier mobility values,[27] hence, high performance. Unfortunately, high temperatures are not compatible with the polymer reservoirs described above. To maintain thermal compatibility of the polymer reservoir with the In_2O_3, an In_2O_3 nanoparticle ink that only requires a post-deposition drying temperature of 100°C is introduced. For planar EGT, the feasibility of In_2O_3 nanoparticle used as channel material has previously been demonstrated.[28,29] Nevertheless, the achieved mobility values are about a factor of ten lower compared to the previously discussed In_2O_3 precursor ink,[28] which requires high annealing temperatures though.

**ADVANCED
SCIENCE NEWS**

www.advancedsciencenews.com

**ADVANCED
MATERIALS
TECHNOLOGIES**

www.advmattechnol.de

Figure 3. Surface morphology of an In_2O_3 nanoparticle droplet with a surface roughness of 30 nm. a) 2D and b) 3D AFM image of inkjet printed In_2O_3 nanoparticle film.

The preparation of the In_2O_3 nanoparticle ink is straightforward. Commercially available In_2O_3 nanoparticles are loaded into double-deionized water and stabilized with the help of poly(acrylic acid) sodium salt (PAANa). The PAANa ligands adsorb to the surface of the nanoparticles and change their surface energy as well as steric properties, decreasing the agglomeration probability.[28] The stabilizer is required to avoid that the nanoparticles agglomerate before loading into the printer cartridge. However, after printing it is necessary that the nanoparticles agglomerate to form a semiconducting film where charge carriers can percolate. For that reason, a flocculation agent is added prior to printing to the In_2O_3 nanoparticle solution in order to remove the PAANa ligands. This supports the densification of the In_2O_3 nanoparticles, improving the film quality.[28] Unfortunately, the flocculation agent can have a negative influence on the electrical characteristics of the EGTs. Previous works have shown that 20 mM sodium chloride, as flocculation agent, is sufficient to improve the film quality while having a negligible influence on the EGT's electrical performance.[28,30] The particle size of the In_2O_3 is between 30 and 70 nm. However, agglomerates bigger than 150 nm can be found after printing which is the result of the flocculation agent that is added to support the formation of the semiconducting film. **Figure 3** shows the surface morphology of an inkjet printed In_2O_3 nanoparticle droplet, based on AFM. Thus, root mean square (RMS) of the surface roughness is measured to be ≈30 nm.

2.3. Electrolyte-Gated Transistors Printed into Polymer Reservoirs

The previous discussed reservoir and In_2O_3 nanoparticles are used to fabricate EGTs. Thereby, the materials that pertain to the EGT stack are printed inside the reservoir. The $W_{channel}/L_{channel}$-ratio is 90 µm/3 µm and defined by the geometry and the gap present at the bottom of the reservoir. **Figure 4** shows the microscope image of the EGT. The two black rectangles are the drain- and source-electrodes and the gap is the channel region of the EGT.
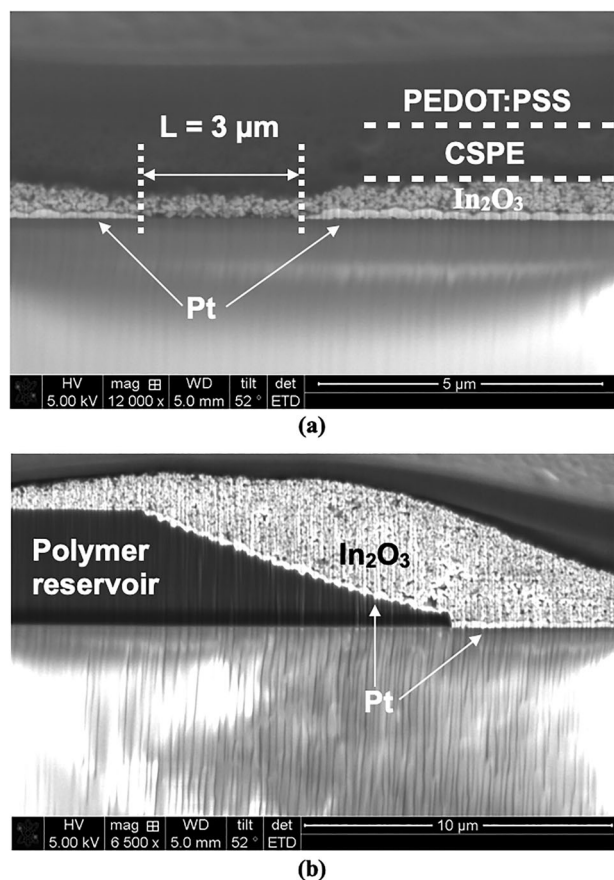
Next, the In_2O_3 nanoparticle based ink is printed into the reservoir. After a drying step at 100°C for 15 min, a 2 µm thick In_2O_3 film is observed at the middle of the reservoir (**Figure 5**a). Due to the coffee ring effect, the thickness of the In_2O_3 film can be
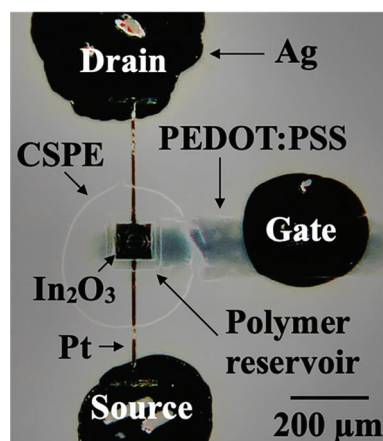
Figure 4. Microscope image of the studied electrolyte-gated field-effect transistor printed into a 3D polymer reservoir with Pt based inner sidewalls.

up to 5 µm at the edges of the reservoir (Figure 5b). Following the In_2O_3 film, a composite solid electrolyte (CSPE) is printed into the reservoir on top of the indium oxide. The CSPE helps to reduce the supply voltage requirements down to 1 V. Depending on the applied gate potential, two Electronic Double Layers (EDLs), known as the Helmholtz Double Layer, are established at the gate/CSPE and CSPE/semiconductor interfaces. The EDL assists in accumulating and repelling charge carriers at the surface of the semiconductor,[31] hence, being responsible for the gate modulation of the EGT. As the last printing step, PEDOT:PSS is printed on top of the CSPE and extended outside to the gate contact pad. Therefore, the PEDOT:PSS is the top-gate electrode of the transistor. Figure 4 shows a microscope image of the EGT. The height map (Figure S4, Supporting Information) shows that the maximum height of the EGT is 6 µm.

The transfer and output curves of the EGT with In_2O_3 nanoparticle channel are shown in **Figure 6**. The key parameters of the transistor are extracted from the transfer curve at a drain-source voltage (V_{ds}) of 1 V. In this regard, the on-current is read at the maximum gate-source voltage (V_{gs}) of 1 V and is ≈148 µA. On the other hand, the minimum drain-source current (I_{ds}), flowing at V_{gs} = 1 V is considered to be the off-current. With the help of

**ADVANCED
SCIENCE NEWS**

www.advancedsciencenews.com

**ADVANCED
MATERIALS
TECHNOLOGIES**

www.advmattechnol.de

Figure 5. Cross-sectional FIB/SEM images of the electrolyte-gated transistor integrated into a 3D reservoir. A 100 μm window was opened with a FIB ThermoFisher STRATA 400 STEM within the center of the reservoir. a) Channel region of the transistor with a channel length of 3 μm. b) In_2O_3 nanoparticles accumulate at the edge of the reservoir due to the coffee-ring effect.

Figure 6b, we deduce the off-current to be 5.2 nA, which yields an on/off-ratio of $\approx 2.8 \times 10.^4$ This means that the I_{ds} current rises by at least over four orders of magnitude. This aspect is important in digital applications in order to be robust against noise. Furthermore, at a threshold voltage (V_{th}) of −312 mV, charge carriers start to accumulate at the surface of the channel, establishing a conductive path between the source- and the drain-electrodes. The threshold voltage is extracted via the square root method.[32] As can be seen from Figure 6, the threshold voltage is negative which indicates that a large number of free charge carriers are available to drive a current between the drain- and source-electrodes. In metal-oxides, the large number of free charge carriers is attributed to oxygen vacancies and can be suppressed by doping the semiconductor.[33] Doing so will shift the threshold voltage toward positive values, which is desirable for logic circuit applications. The large number of free charge carriers also has as consequence that an EDL needs to be established to repeal the charge carriers between the source-drain-electrode. This is achieved by a negative V_{gs}, demonstrating that the threshold voltage is in fact negative. Moreover, the sub-threshold slope (S) is with a value of 176 mV dec^{-1} rather high.

3. Conclusion

In summary, a multi-material laser writing technique is used to fabricate polymer reservoirs with conductive structures on it. This reservoir is used to fabricate a fully printed electrolyte-gated field-effect transistor (EGT) with indium oxide (In_2O_3) channel. Thereby, the 3D reservoir structure helps to confine the printed functional inks, even if deposited on structures below 10 μm. In addition, the reservoir itself acts as drain- and source electrode improving the electrical contact between the channel and metallic electrode due to the large contact area. However, the presented EGT shows a reasonable on/off-ratio of $\approx 2.8 \times 10^4$ with leakage currents below 10 pA. Therefore, this concept can be used to realize novel types of devices in printed electronics and bioelectronics wherein it might, e.g., be important to confine solvents within a defined area or volume in order to be analyzed.
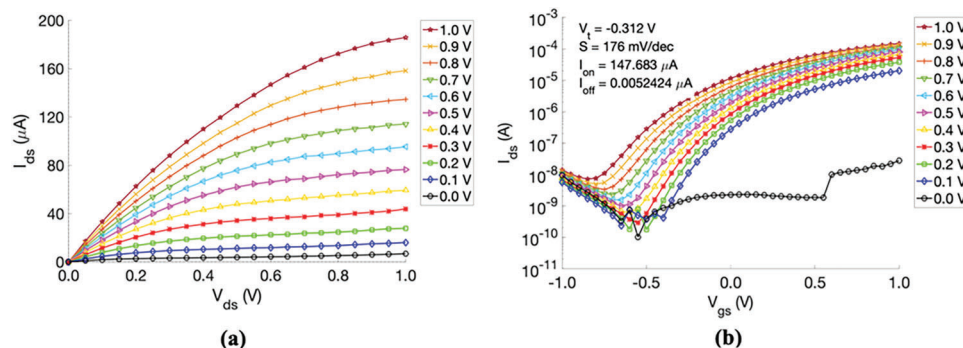
4. Experimental Section

Photoresist: For the printing of polymer reservoir, photoinitiator 7-Diethylamino-3-thenoylcoumarin (DETC, Exciton) was dissolved into pentaerythritol triacrylate (PETA, Sigma–Aldrich) with concentrations of 0.25 wt.%.

Pt Ink: A 0.5 M stock solution of ammonium iron oxalate trihydrate (($NH4)_3[Fe(C2O4)_3]\cdot 3\ H_2O$, Alfa Aesar, 98%), and a 0.07 M stock solution of ammonium tetrachloroplatinate (($NH4)_2[PtCl_4]$, Alfa Aesar, 99.9% metal basis) in deionized water were prepared and stored in the dark at 4 °C. The Platinum ink was always freshly prepared prior to the laser printing of conductive Pt structures by mixing above two stock solutions with a volume ration of 1:1.

Sample Preparation: Precision cover glasses were used as the substrate for the printing of 3D structures, which were first carefully cleaned with water, acetone, isopropanol successively. After that, the cover glasses were kept in an oven at 150 °C for 1 h to remove water on the surface and treated with oxygen plasma for 10 min. Then, the cleaned cover glasses were salinized by a solution of (3-aminopropyl) triethoxysilane dissolved in toluene (0.2% vol) for 60 min at ambient temperature. After washing successively with toluene, acetone, isopropanol, and drying with nitrogen, the cover glasses were ready for use. Prior to laser printing, a polydimethylsiloxane (PDMS) ring with a height of $\approx$1 mm was attached to the glass surface as a reservoir for both photoresist and Pt ink. In Pt printing process, the top of PDMS reservoir was covered with a second PDMS piece to prevent any evaporation of solvent during the fabrication process.

Laser Printing: A Ti:Sa femtosecond laser (Coherent Chameleon Ultra II) was used for both multi-photon polymerization of photoresist and multi-photon reduction of Pt. The laser source was first focused into photoresist by an oil objective lens (Zeiss Plan-Apochromat 63×/1.4, numerical aperture NA = 1.4), which was mounted by a piezoelectric stage (Physik Instrumente P-733.ZCL) with 100 μm travel to translate the focus along the optical axis. The sample was translated horizontally using a 2D piezo stage (Physik Instrumente P-734.2CL) with 100 μm × 100 μm travel. The 2D stage was mounted on top of another stage (Physik Instrumente P-M-686) with 25 mm × 25 mm travel for coarse movement. 3D polymer structures were printed by a computer controlled relative scanning of the laser focus in a photoresist with computer. After printing was completed, the samples were developed for 10 min in isopropanol and subsequently blown dry with nitrogen gas. After that, the printed polymer structures were immersed in Pt ink. The laser source was then focused onto the existing polymer structure by water objective lens (Zeiss LD C-APOCHROMAT 100×/1.25 W, numerical aperture NA = 1.25). Designed 3D Pt patterns were printed on the surface of glass and existing polymer structure. An additional dedicated continuous-wave diode laser (operating at 675 nm wavelength) was used to find the z-position of the glass-water interface as well as polymer-water interface with high accuracy via a confocal detection

**ADVANCED
SCIENCE NEWS**

www.advancedsciencenews.com

**ADVANCED
MATERIALS
TECHNOLOGIES**

www.advmattechnol.de

Figure 6. Electrical characteristics of the printed electrolyte-gated field-effect transistor (EGT) integrated into a 3D polymer reservoir. The Pt coated inner sidewalls, that are separated through a gap, act as the drain- and source-electrodes. a) Output and b) transfer curves of the EGT.

scheme. After the writing was completed, the samples were washed for 5 min in pure water and blown dry gently with nitrogen gas. During the printing procedure, an acousto-optic modulators (AOMs, AA Opto Electronic MTS40-A3–750.850) was used to modulate the power of focused femto second (fs) laser. A camera and an illumination by a red light-emitting diode in transmission by a red light-emitting diode were used to monitor the exposure process in situ.

Structure Characterization: The surface morphologies of the samples were measured on a Zeiss Leo 1530 scanning electron microscope operating at 10.0 keV. The samples were coated with an 8 nm gold layer prior to measurements.

Nanoparticle Ink Preparation: To mix the semiconducting ink, In_2O_3 nanoparticles purchased from Chempur GmbH were added to double-distilled water. The loading of the In_2O_3 nanoparticles was 10 wt.% and poly acrylic acid (PAANa), purchased from Sigma–Aldrich, was added to the dispersion as the stabilizer. The loading of the PAANa stabilizer was 10 wt.% of the nanoparticles. Next, a pearl mill (Dispermat) was used to prepare the nanodispersion ink. As grinding media, 0.2–0.3 mm zirconia pearls was added to the ink to break large agglomerates. The mixture was spun for 90 min at rotational speed of 6000 rpm. Afterward, the zirconia pearls were removed through consecutive filtration steps with syringe filters in the size of 5, 0.45, and 0.2 μm, respectively. Before printing, 20 mmol of sodium chloride (NaCl) was added to the solution to destabilize the solution and to support the re-agglomeration in order to form a high-quality film.

Composite Solid Polymer Electrolyte Preparation: The composite solid polymer electrolyte (CSPE) was based on 6 g dimethyl sulfoxide (DMSO), 0.3 g poly(vinyl alcohol) (PVA), 0.63 g propylene carbonate (PC), and lithium perchlorate (LiClO$_4$) all purchased at Sigma–Aldrich. Thereby, the PVA was dissolved in DMSO for 60 min at 90°C. The LiClO4 was dissolved in PC for 60 min at room temperature. Next, both dispersions were mixed together for 12 h at room temperature. Prior to printing, the CSPE ink was filtered through a 0.2 μm syringe filter.

PEDOT:PSS Preparation: PEDOT:PSS (Poly-(3,4-ethylendioxythiophen)-poly-(styrolsulfonat) in H$_2$O, high-conductivity grade, Sigma–Aldrich) was mixed with ethyleneglycol (1,2-Ethandiol, Glykol, Sigma–Aldrich) in a ratio of 97 and 3 wt.%, respectively, for 60 min at room temperature. The mixture was then filtered through a 0.45 μm filter.

Transistor Printing: First, Ag ink (Smart'Ink S-CS01130, Sigma–Aldrich) was printed with the help of the Fujifilm Dimatix Materials inkjet printer (DMP 2831) to form the gate, drain, and source contact pads. Following, the In_2O_3 nanoparticles are inkjet printed into the polymer reservoir. After drying the printed In_2O_3 film for 30 min at 100°C, the CSPE was inkjet printed on top of the reservoir at a temperature of 40°C. Finally, the PEDOT:PSS solution was inkjet printed on top of the reservoir at a temperature of 50 C and extended to the gate contact pad.

Electrical Characterization: This was how the transistors were characterized. Electrical measurements were performed with a Agilent 4146C

semiconductor parameter analyzer where the transistors were electrically contacted through a Süss MicroTec EP6 probe station.

Electron Microscopic Characterization: Cross-sectional samples of the material were cut and analyzed using a FIB/SEM cross-beam instrument (STRATA 400 STEM, ThermoFisherScientific) at 30 and 5 kV acceleration voltages for ion beam and electron beam respectively. Cutting was performed with a Ga-ion beam using beam currents starting from 21 to 9 nA for overview-cuts and 93 pA for detailed cross-sections at higher magnification (Figure 5).

Supporting Information

Supporting Information is available from the Wiley Online Library or from the author.

Conflict of Interest

The authors declare no conflict of interest.

Data Availability Statement

The data that support the findings of this study are openly available in Radar4KIT at https://doi.org/10.35097/939, reference number 939.

[1] P. Martins, N. Pereira, A. C. Lima, A. Garcia, C. Mendes-Filipe, R. Policia, V. Correia, S. Lanceros-Mendez, *Adv. Funct. Mater.* **2023**, *33*, 2213744.

[2] Y. Khan, A. Thielens, S. Muin, J. Ting, C. Baumbauer, A. C. Arias, *Adv. Mater.* **2020**, *32*, 1905279.

[3] K. Suganuma, *Introduction to Printed Electronics*, Springer, New York, NY **2014**.

[4] M. Berggren, D. Nilsson, N. D. Robinson, *Nat. Mater.* **2007**, *6*, 3.

[5] S. M. F. Cruz, L. A. Rocha, J. C. Viana, *Flexible Electronics* **2018**.

[6] V. Beedasy, P. J. Smith, *Materials* **2020**, *13*, 704.

[7] H. W. Tan, Y. Y. C. Choong, C. N. Kuo, H. Y. Low, C. K. Chua, *Prog. Mater. Sci.* **2022**, *127*, 100945.

[8] J. Perelaer, P. J. Smith, D. Mager, D. Soltman, S. K. Volkman, V. Subramanian, J. G. Korvink, U. S. Schubert, *J. Mater. Chem.* **2010**, *20*, 8446.

[9] M. W. Park, D.-Y. Kim, U. An, J. Jang, J.-H. Bae, I. M. Kang, S.-H. Lee, *ACS Appl. Mater. Interfaces* **2022**, *14*, 46819.

[10] T. Granlund, T. Nyberg, L. Stolz Roman, M. Svensson, O. Inganäs, *Adv. Mater.* **2000**, *12*, 269.

[11] A. Mahajan, W. J. Hyun, S. B. Walker, G. A. Rojas, J.-H. Choi, J. A. Lewis, L. F. Francis, C. D. Frisbie, *Adv. Electron. Mater.* **2015**, *1*, 1500137.

[12] K. S. Jochem, P. Kolliopoulos, C. D. Frisbie, L. F. Francis, *Flexible Printed Electron.* **2021**, *6*, 045005.

[13] L. Hirt, A. Reiser, R. Spolenak, T. Zambelli, *Adv. Mater.* **2017**, *29*, 1604211.

[14] S. Maruo, O. Nakamura, S. Kawata, *Opt. Lett.* **1997**, *22*, 132.

[15] V. Hahn, F. Mayer, M. Thiel, M. Wegener, *Opt. Photonics News.* **2019**, *30*, 28.

[16] L. Wang, I. Meric, P. Y. Huang, Q. Gao, Y. Gao, H. Tran, T. Taniguchi, K. Watanabe, L. M. Campos, D. A. Muller, J. Guo, P. Kim, J. Hone, K. L. Shepard, C. R. Dean, *Science* **2013**, *342*, 614.

[17] M. S. Choi, N. Ali, T. D. Ngo, H. Choi, B. Oh, H. Yang, W. J. Yoo, *Adv. Mater.* **2022**, *34*, 2202408.

[18] D. H. Kim, K.-H. Lee, S. H. Lee, J. Kim, J. Yang, J. Kim, S.-I. Cho, K. H. Ji, C.-S. Hwang, S.-H. Ko Park, *IEEE Electron Device Lett.* **2022**, *43*, 1677.

[19] L. Yang, A. Rahimzadegan, V. Hahn, E. Blasco, C. Rockstuhl, M. Wegener, *Laser Photonics Rev.* **2022**, *16*, 2100411.

[20] L. D. Zarzar, B. S. Swartzentruber, J. C. Harper, D. R. Dunphy, C. J. Brinker, J. Aizenberg, B. Kaehr, *J.Am. Chem. Soc.* **2012**, *134*, 4007.

[21] S. Hashimoto, D. Werner, T. Uwada, *J. Photoch. Photobio.,C* **2012**, *13*, 28.

[22] L. Yang, F. Mayer, U. H. F. Bunz, E. Blasco, M. Wegener, *Light: Adv. Manuf.* **2021**, *2*, 296.

[23] O. Bierwagen, *Semicond. Sci. Technol.* **2015**, *30*, 02400.

[24] S.-Y. Han, D.-H. Lee, G. S. Herman, C.-H. Chang, *J. Disp. Technol.* **2009**, *5*, 520.

[25] J. Leppäniemi, O.-H. Huttunen, H. Majumdar, A. Alastalo, *Adv. Mater.* **2015**, *27*, 7168.

[26] S.-Y. Kim, K. Kim, Y. H. Hwang, J. Park, J. Jang, Y. Nam, Y. Kang, M. Kim, H. J. Park, Z. Lee, J. Choi, Y. Kim, S. Jeong, B.-S. Bae, J.-U. Park, *Nanoscale* **2016**, *8*, 17113.

[27] P. Barquinha, R. Martins, L. Pereira, E. Fortunato, *Transparent Oxide Electronics: From Materials to Devices*, John Wiley & Sons, Ltd, Hoboken,NJ **2012**.

[28] T. T. Baby, S. K. Garlapati, S. Dehm, M. Häming, R. Kruk, H. Hahn, S. Dasgupta, *ACS Nano* **2015**, *9*, 3075.

[29] S. Dasgupta, R. Kruk, N. Mechau, H. Hahn, *ACS Nano* **2011**, *5*, 9628.

[30] M. Häming, T. T. Baby, S. K. Garlapati, B. Krause, H. Hahn, S. Dasgupta, L. Weinhardt, C. Heske, *Appl. Surf. Sci.* **2017**, *396*, 912.

[31] X. Feng, G. C. Marques, F. Rasheed, M. B. Tahoori, J. Aghassi-Hagmann, *IEEE Trans. Electron Devices* **2019**, *66*, 5272.

[32] A. Ortiz-Conde, F. J. García-Sánchez, J. Muci, A. Terán Barrios, J. J. Liou, C.-S. Ho, *Microelectr. Reliab.* **2013**, *53*, 90.

[33] G. Yang, H. Tian, Z. Yu, T. Huang, Y. Xu, H. Sun, W. Sun, W. Wu, *IEEE Electron Device Lett.* **2022**, *43*, 1898.